(41) Ballard, D. G. H. In ref 5, p 233.
(42) Ballard, D. G. H., et al. U.S. Patent 3,969,386, 1976.
(43) Cardinelli, J. P.; et al. Patent, Ger. Offen. 2,653,379, June 2, 1977.
(44) Setterquist, R. A. U.S. Patent 3,950,269, 1976.
(45) Setterquist, R. A.; Tebbe, F. N.; Peet, W. G. *Polym. Sci. Technol.* **1983**, *19*, 167.
(46) Peet, W. G.; Tebbe, F. N.; Setterquist, R. A.; Parshall, G. W. In *Coordination Polymerization*; Price, C. C., Vanderberg, E. J., Eds.; Plenum Press: New York, 1983.
(47) Setterquist, R. A. U.S. Patent 3,932,307, Jan 13, 1976.
(48) Setterquist, R. A. U.S. Patent 4,017,525, April 12, 1977.
(49) Setterquist, R. A. U.S. Patent 3.971,767, July 27, 1976.
(50) Firment, L. E. *J. Catal.* **1982**, *77*, 491; **1983**, *82*, 196.
(51) Wunderlich, B. *Macromolecular Physics*; Academic Press: New York, 1976; Vol. II; and private conversation.
(52) Luongo, J. P. *J. Appl. Polym. Sci.* **1960**, *3*, 302.
(53) Tullock, C. W.; Tebbe, F. N.; Mulhaupt, R.; Ovenall, D. W.; Setterquist, R. A.; Ittel, S. D., submitted for publication in *Polym. Sci.*
(54) Collette, J. W.; Tullock, C. W. U.S. Patent 4,298,722, Nov 3, 1981.

Elastomeric Polypropylenes from Alumina-Supported Tetraalkyl Group IVB Catalysts. 2. Chain Microstructure, Crystallinity, and Morphology

John W. Collette,* Derick W. Ovenall, Warren H. Buck, and Raymond C. Ferguson†

Central Research and Development Department‡ and Plastics Products and Resins Department, E. I. du Pont de Nemours & Co., Inc., Experimental Station, Wilmington, Delaware 19898. *Received August 29, 1988; Revised Manuscript Received February 27, 1989*

ABSTRACT: Elastomeric polypropylene (ELPP)[1] and its components, separated by solvent extraction, have been characterized by NMR and IR spectroscopy, differential scanning calorimetry, size-exclusion chromatography, X-ray diffraction, nitric acid etching, and electron microscopy. The chain microstructure of ELPP is stereoblock, consisting of alternating isotactic and stereoirregular sequences, described approximately by second-order Markov polymerization statistics, which were used to calculate the distribution of isotactic block lengths. The results confirm that the high molecular weight ELPP fractions of low stereoregularity have isotactic blocks that cocrystallize with the more isotactic components to form an elastomeric network. The morphology consists of cocontinuous hard and soft phases, of crystalline isotactic and amorphous atactic polypropylene, respectively.

Background

In part 1, we reported the synthesis of a novel elastomeric polypropylene (ELPP) made by polymerizing propylene with highly active heterogeneous zirconium catalysts.[1] The elastic properties depend predominantly on the molecular weight of the ether-soluble ELPP fractions, while the strength and stiffness correlate with the total polymer crystallinity. According to our hypothesis, the isotactic segments of the ether-soluble ELPP cocrystallize with the larger isotactic blocks of the more stereoregular ELPP components, forming an elastic network.

In this paper, we explore further the origins of the elastomeric properties and structure–property relationships of ELPP by study of the chain microstructure, crystallinity, and morphology of components separated by solvent fractionation.

Experimental Section

Extraction. ELPP was separated by successive extraction of extruded blown film or extruded pellets with solvents of increasing boiling temperature, usually ether and hexane or heptane. Standard unjacketed Soxhlet extractors with 500-mL capacity tubes were used. The samples were blanketed with nitrogen during extraction. Extractions were continued until evaporation of the solvent showed that a negligible amount of polymer was extracted during a 24-h period, then extraction was continued with the next higher boiling solvent. The fractions were recovered by solvent evaporation.

NMR. Solutions of the polymers (10% w/v) were prepared in dideuteriotetrachloroethane or in 1:1 mixtures of $C_2D_2Cl_4$ with *o*-dichlorobenzene, containing 0.1% 2,6-di-*tert*-butyl-4-methylphenol (BHT) as a stabilizer. Proton-decoupled ^{13}C NMR spectra were measured with Bruker WH90 and WM400 spectrometers operating at 22.63 and 100.6 MHz, respectively, at sample temperatures of 120–145 °C. Differential saturation of the peaks was avoided by a 10-s delay between 90° pulses. The central peak of $C_2D_2Cl_4$ was taken as 74.14 ppm.

IR. A Nicolet FTIR spectrometer was used to obtain infrared spectra on melt-pressed films by transmission. The absorbances of the 997- and 993-cm^{-1} bands were used to calculate the IR ratio, A_{997}/A_{973}, a measure of the isotactic helix content.[2] Note that we employ the inverse of the ratio used by Luongo, because it correlates linearly with estimates of crystallinity by DSC, X-ray diffraction, and density measurements.

Test Specimens. All ELPP samples and fractions were compression molded by heating in a press under light pressure. The ether-soluble fractions were heated to 80 °C and all others to 180 °C for 10 min, then cooling water was run through the press platens, as full ram pressure of 276 MPa was applied and held until the platens were at room temperature.

DSC. Differential scanning calorimetry measurements of the test specimens were performed on a Du Pont 1090 thermal analyzer using a Du Pont 912 dual sample DSC module at a heating rate of 10 °C/min. The percent crystallinity, $100\Delta H_f/\Delta H_f°$, was calculated from the observed heat of fusion, ΔH_f, and $\Delta H_f° = 209$ J/g, the heat of fusion of crystalline polypropylene.[3]

X-ray. X-ray diffraction patterns of the specimens were obtained on a scanning diffractometer with Ni-filtered Cu Kα radiation. Crystallinity was calculated from the areas under the crystalline peaks versus the total scattering.

Density. Density crystallinity was measured by a buoyancy method with methanol as the buoyant medium. Five replicate measurements were made for each sample. The results were

† Present address: Condux, Inc., 300 Whitby Dr., Wilmington, DE 19803.
‡ Contribution No. 4822.

0024-9297/89/2222-3858$01.50/0

Table I
Percent Head-to-Head in Polypropylene Solvent Fractions

catalyst	$TiCl_4/AlEt_3$	$TNZ/Al_2O_3/H_2$
whole polymer	4	3
acetone sol.	7	nd[a]
ether sol.	5	6
hexane sol.	4	2
hexane insol	0	0

[a] nd = not determined.

corrected for residual alumina catalyst determined by ashing the samples at 800 °C for 2 h. Densities of crystalline polypropylene, amorphous polypropylene, and alumina were taken as 0.938, 0.852, and 3.97 g/cm^3, respectively.

Electron Microscopy. Replicas for transmission electron microscopy (TEM) were prepared by fracturing a small piece of test specimen, which had been frozen in liquid nitrogen, in a VEECO high-vacuum evaporator at a pressure of about 130 μPa ($\sim 1 \times 10^{-6}$ mmHg). The sample was cooled with liquid nitrogen while being shadowed with evaporated Pt/C and then was coated with a thin film of evaporated C. Replicas were removed from the polymer substrate by dissolving the polymer in hot 1,2,4-trichlorobenzene and then picking up the replica fragments from the surface with a 200-mesh Cu microscope grid. Argon ion etching was performed under the following conditions: 1000 VAC potential between electrodes, 500 cm^3/min Ar flow rate, 1-cm electrode separation, and electrode temperature approximately 0–3 °C. Electron micrographs were made with a Zeiss EM-9A microscope.

Nitric acid degradation was carried out in 200-mL round-bottom flasks to which 100 mL of nitric acid (bp 120 °C) or fuming nitric acid (bp 130 °C) had been added. The acid was heated to reflux; approximately 2 g of polymer granules were added and etched at reflux for 1–3 h. The polymer was recovered by diluting the acid with 200 mL of distilled water and then filtering this mixture through glass thimbles containing coarse fritted discs. The thimbles containing the etch residue were then Soxhlet extracted with water for about 4 h and then with acetone for 2 h. Molecular weight distributions of the etched samples were determined by gel permeation chromatography as described in Part 1.[1]

Results and Discussion

NMR: Chain Microstructure. The regioregularity and stereoregularity of the chain microstructure of ELPP and fractions were estimated from the ^{13}C solution spectra. Regioisomerism in ELPP, i.e., inverted enchainment of monomer units, is revealed by relatively weak resonances not attributable to head-to-tail addition. These have been observed and tentative partial assignments made by Asakura et al.[4] The empirical formulas of Lindeman and Adams for the shifts of alkanes[5] and other additivity rules for polyolefins[6] predict shifts in the regions where these weak resonances are observed, i.e., 31–39 ppm for methylene and methine carbons and 16–17 ppm for methyl carbons in head-to-head and tail-to-tail sequences. Consistent assignments for the methylene and methine carbons could not be made, partly because tacticity effects were apparent and not fully understood. We assigned resonances at 17.4, 17.1, and 15.2 ppm to vicinal dimethyl carbons, and the intensities were used to estimate the fraction of inversions.

Typical ELPP samples had less than 5% inverted propylene units, indicating that the regioselectivity of the TNZ/Al_2O_3 catalyst is high. Regiosequence irregularities occurred predominantly in the ether-soluble and hexane-soluble fractions, with a pattern similar to that of a polymer made with a low stereospecific $TiCl_4/AlEt_3$ catalyst (Table I).

Figure 1 reveals the structural inhomogeneity of ELPP and solvent fractionation based on chain microstructure. The nine features of the head-to-tail methyl resonance pattern have been assigned to the 10 possible pentad steric

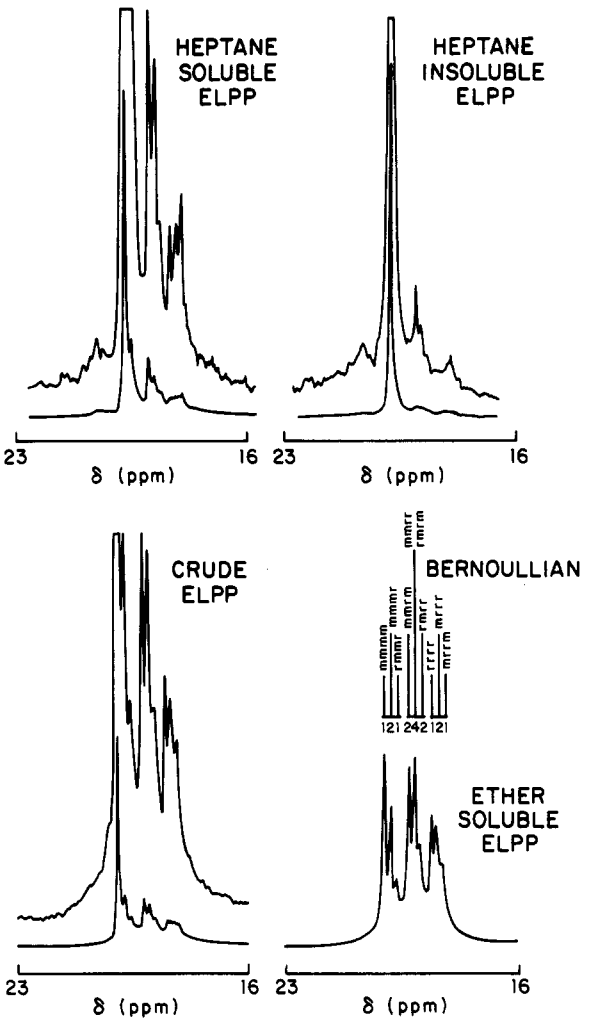

Figure 1. Methyl region of 100.6-MHz proton-decoupled ^{13}C NMR spectra of ELPP and fractions, 10% w/v polymer in $C_2D_2Cl_4$ at 120 °C, internally referenced to the solvent peak at 74.14 ppm. Fractions from boiling hexane extractions have similar, but not quantitatively identical, patterns. The pentad assignments and intensity distribution for random tacticity, Bernoullian $P(m) = 0.5$, are shown in the inset.

Table II
Chemical Shifts of ^{13}C Methyl Resonances of Polypropylenes

head-to-tail pentads	chem shift, ppm[a]	head-to-tail pentads	chem shift, ppm[a]
mmmm	21.67	*mrmr*	20.55
mmmr	21.44	*rrrr*	20.19
rmmr	21.24	*rrrm*	20.07
mmrr	20.90	*mrrm*	19.88
mrmm + *rmrr*	20.72	vicinal dimethyl (head-to-head)	15.2, 17.1, 17.4

[a] 10% solutions in dideuteriotetrachloroethane at 145 °C. Reference, solvent peak at 74.14 ppm.

arrangements[7,8] given in Table II.

The isotacticity of ELPP fractions, as measured by the *mmmm* pentads, increased with each successive fraction and reached ca. 70% in the hexane- or heptane-insoluble fractions. The steric defects in the insoluble fractions were mainly of the type *mmmmrrmmmm*, also observed in more conventional titanium-catalyzed polypropylenes. Our data show that *mmmm* > *mmmr* = 2*mrrm*, consistent with the presence of such defects as observed by Zambelli et al.[9] and Doi.[10] Predominance of these defects indicates that a steric error from a faulty insertion is not perpetuated, i.e., the asymmetric placements are *llldlll*, not *llldddl*. This

suggests further that steric control is determined by the catalytically active metal complex. The hexane-insoluble fractions of ELPP still contain considerable amounts of atactic sequences; this probably results from incomplete separation of the different stereoisomers in the solvent extraction.

To develop and test statistical models of the sequence distributions, the NMR triad distributions were calculated from the observed pentad distributions by the relationships[11]

$$[mm] = [mmmm] + [mmmr] + [rmmr] \quad (1)$$

$$[mr] = [mmrr] + [rrmr] + [mrmr] + [mmrm] \quad (2)$$

$$[rr] = [mrrm] + [mrrr] + [rrrr] \quad (3)$$

First-order Markov probabilities were calculated from the NMR triad data as follows:

$$P(m/r) = [mr]/(2[mm] + [mr]) \quad (4)$$

$$P(r/m) = [mr]/(2[rr] + [mr]) \quad (5)$$

where $P(m/r)$ is the probability that a polymer chain ending in two units having the same configuration (meso) adds a monomer unit to give the opposite configuration (racemic) and $P(r/m)$ that an m follows an r.[11]

For all ELPP samples and fractions examined, $P(m/r) + P(r/m) < 1$, indicating that Bernoullian statistics, for which the sum = 1, did not apply. First-order Markov statistics also did not fit the observed pentad intensities; thus, higher order statistics or a stereoblock model were required.

Second-order Markov statistics were estimated for ELPP and its fractions. In this case, the configuration of the last two diads affects the probability that the next propylene unit will be incorporated to form a new meso or racemic diad. The validity of second-order Markov statistics was first tested analytically with relationships derived from the explicit expressions for the pentad probabilities (ref 11, p 159). The ratios of some pairs of pentad probabilities are functions of single placement probabilities, as follows:

$$P(mm/m) = 2R_1/(1 + 2R_1) = 2R_2/(2 + R_2) \quad (6)$$

where $R_1 = [mmmm]/[mmmr]$ and $R_2 = [mmmr]/[rmmr]$

$$P(rr/m) = 1/(1 + 2R_3) = 2/(2 + R_4) \quad (7)$$

where $R_3 = [rrrr]/[rrrm]$, $R_4 = [rrrm]/[mrrm]$, $P(mm/m)$ is the probability that a growing polymer chain ending in an mm sequence will add the next unit to form an mmm sequence, and $P(rr/m)$ is the probability that a chain ending rr will form an rrm sequence.

If the placement probabilities calculated from the observed pentad intensity ratios agreed within experimental error, computer simulations were used to obtain the best estimates of all four independent placement probabilities, $P(mm/m)$, $P(mr/m)$, $P(rm/m)$, and $P(rr/m)$, starting with the estimates from eq 6 and 7. The distributions were calculated with a computer program originally developed by Harwood.[12]

Tests using eq 6 and 7 indicated that second-order Markov statistics could not fit the pentad distributions of the whole polymers and the ether-soluble fractions. Satisfactory matches were obtained for the hexane-soluble and hexane-insoluble fractions. Representative results are given in Table III.

Differences in the probabilities for the fractions suggest activity of two or more sites of differing stereoregulating character. Pentad statistics do not provide an adequate basis for testing multiple-site models, so we used only second-order Markov approximations.

Table III
Second-Order Markov Statistics for ELPP Fractions

fraction	$P(mm/m)$	$P(mr/m)$	$P(rm/m)$	$P(rr/m)$
hexane insol	0.92	0.5	0.9	0.9
hexane sol.	0.85	0.4	0.7	0.4
ether sol.	0.70[a]	na[b]	na[b]	na[b]

[a] Second-order Markov statistics gave poor fits to the ether-soluble fraction and whole polymer. [b] na, not applicable. Observed intensity ratios inconsistent with eq 6 and 7.

Table IV
ELPP Crystallinity and Molecular Weight

fraction	η_{inh},[a] dL/g	IR ratio,[b] %	X-ray, %	density,[c] %
ELPP 1, whole	2.70	38	21	19
ether sol.	0.73	16	8	0
hexane sol.	2.56	26	14	17
hexane insol	4.16	53	29	44
ELPP 2, whole	5.43	38	21	23
ether sol.	2.12	18	9	0
hexane sol.	3.90	23	12	13
hexane insol	8.72	58	32	42
ELPP 3, whole	12.1	31	17	24
ether sol.	3.42	18	9	9
hexane sol.	7.80	28	15	25
hexane insol	10.8[d]	40	22	29

[a] Inherent viscosity of 0.05 g/dL solution in decahydronaphthalene, stabilized with BHT, at 135 °C. [b] IR ratio, A_{997}/A_{973} (cm^{-1}), expressed as a percentage. [c] Density measured in methanol at 23 °C, mean of five determinations. [d] No antioxidant used; some degradation possible.

^{13}C NMR was also used to correlate the $mmmm$ pentad intensity with the crystallinity of ELPP and its fractions. When an ELPP solution was measured at 135 °C, all segments of the polymer contributed to the methyl pentad resonances. After the sample was cooled to room temperature and held there for at least 24 h, the relative intensity of the $mmmm$ pentad intensity decreased significantly in the spectrum measured at ca. 27 °C (Figure 3). This is attributed to immobilization of predominantly isotactic polymer blocks by crystallization, which broadens resonances due to incomplete averaging of their chemical shift tensors and dipole interactions.

Assuming that the chain segments in the amorphous solvent-swollen phase remained mobile and that the nonisotactic pentad pattern was largely insensitive to the temperature change, the decrease in relative $mmmm$ intensity is a measure of the fraction of polymer crystallized. An NMR rigidity parameter defined as

$$R_{NMR} = F_h - F_l(1 - F_h)/(1 - F_l) \quad (8)$$

expresses the decrease as a fraction of the total pentad resonance intensity. F_h and F_l are the $mmmm$ pentad fractions at the higher and lower temperatures, respectively; the correction term, $(1 - F_h)/(1 - F_l)$, adjusts the nonisotactic pattern intensity to the same absolute value at the two temperatures. Although R_{NMR} is not a direct measure of isotacticity or crystallinity, it provided an estimate of the crystallizable isotactic fraction, which correlated with other estimates of isotacticity and crystallinity.

Crystallinity Estimates. Crystallinity and crystallite sizes were estimated by several complementary techniques, which gave consistent correlations. Crystallinity estimates made by IR, X-ray diffraction, and density are given in Table IV.

Because of ease of measurement, IR was often used to estimate crystallinity via the IR ratio, a measure of the

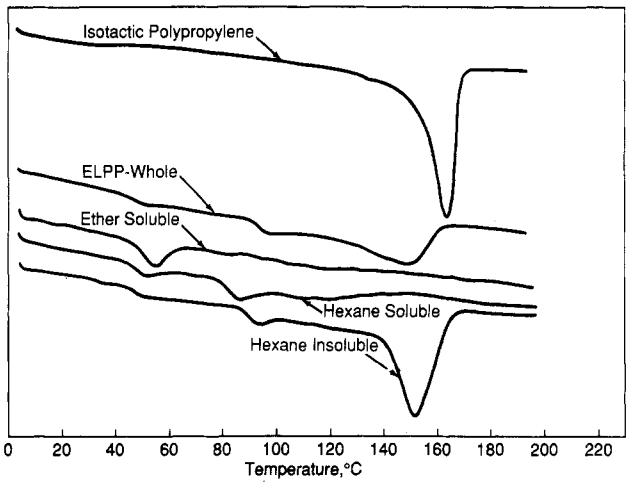

Figure 2. DSC scans of ELPP, solvent fractions and Profax 6523 (highly isotactic) polypropylene. The vertical axes are offset for display purposes.

isotactic helix content. The IR ratio, however, gives neither the true isotactic fraction nor the true percent crystallinity. Randomly coiled isotactic chains do not contribute to the intensity of the "crystalline" band and the intensities of the crystalline bands are insensitive to irregularities in lateral order.[2,13] Moreover, preparation of thin films for transmission measurements gave the IR specimens a different thermal history than the molded test specimens.

X-ray diffraction is more fundamental, but less convenient for quick assays, and was employed only on selected specimens. X-ray crystallinity estimate are subject to difficulties in distinguishing amorphous background scatter from crystalline diffraction. Sample anisotropy, defect crystals, very small crystals, and crystals lacking order in all three dimensions may also affect the estimates.

The density method assumes that a semicrystalline polymer is a two-phase system (crystalline and amorphous) and that the observed sample density can be used to derive the crystallinity, assuming additivity of specific volumes of the two phases. Since the actual structure of a semicrystalline polymer, such as ELPP, is more complicated, containing regions of intermediate density (crystal–amorphous interface, crystal defects), the density crystallinity only approximates the total amount and perfection of the crystalline material.

Differential scanning calorimetry provided independent estimates of crystallinity and information about crystallite sizes and size distribution. Typical DSC scans for ELPP, its fractions, and a commercial crystalline polypropylene are shown in Figure 2. The test specimens all had the same thermal history, except for the ether-soluble fraction, which was molded at 80 °C instead of 180 °C. ELPP and the fractions characteristically had broad melting ranges, from about 20 °C to above 180 °C. The melting temperature of the original polymer and the hexane-soluble fraction were about 150 °C versus 162 °C for commercial crystalline polypropylenes. The glass transitions were in the normal range of ca. −10 °C, well in agreement with data of Cowie et al.[14]

Estimates of crystallinity of ELPP and its fractions were more difficult than for isotactic polypropylene, with its significantly narrower melting range and better defined background. Crystallinities of ELPPs ranged from 2 to 10%, and of hexane-insoluble fractions they were about 30%, compared to about 50% for isotactic polypropylenes.

"Crystallinity", measured by any of the above methods, increased in the order ether soluble, hexane soluble, hexane insoluble. The whole polymer usually had a crystallinity

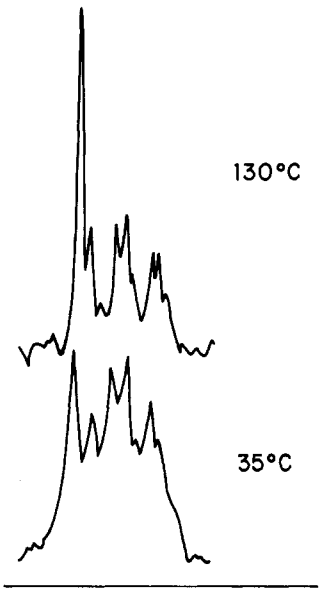

Figure 3. Methyl region of 100.6-MHz proton-decoupled ^{13}C NMR spectra of ELPP. 10% w/v polymer in $C_2D_2Cl_4$ at 130 °C and at 27 °C after cooling at room temperature for 24 h. The strongest peak is the *mmmm* pentad.

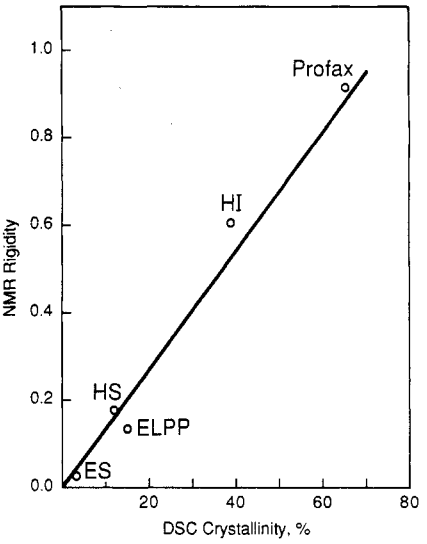

Figure 4. NMR Rigidity versus DSC crystallinity of ELPP fractions and Profax 6523.

between that of the hexane-soluble and hexane-insoluble fractions. Also a linear correlation was observed between the NMR rigidity and DSC crystallinity (R_{NMR} = 0.006 + 0.016 (% crystallinity)) (Figure 4). The results confirmed the presence of isotactic crystallinity in all ELPP fractions.

Each method measures a different physical phenomenon, so quantitative agreement was not expected or found. The IR estimate was always higher than X-ray or density crystallinity, probably because the IR ratio is related to the number of propylene units in isotactic helical placement, whether or not such units are in a crystallite. The IR estimate might be thought of as a "potential crystallinity", while the density and X-ray methods more nearly represent the actual amount of material in crystallites. Short isotactic blocks would contribute to the IR ratio, but not necessarily to the density or X-ray crystallinity, since blocks below some critical chain length are unable to crystallize.

Lamellar Thickness of Crystallites. The sizes of the crystallites, specifically lamellar thicknesses, were determined from DSC data and by transmission electron mi-

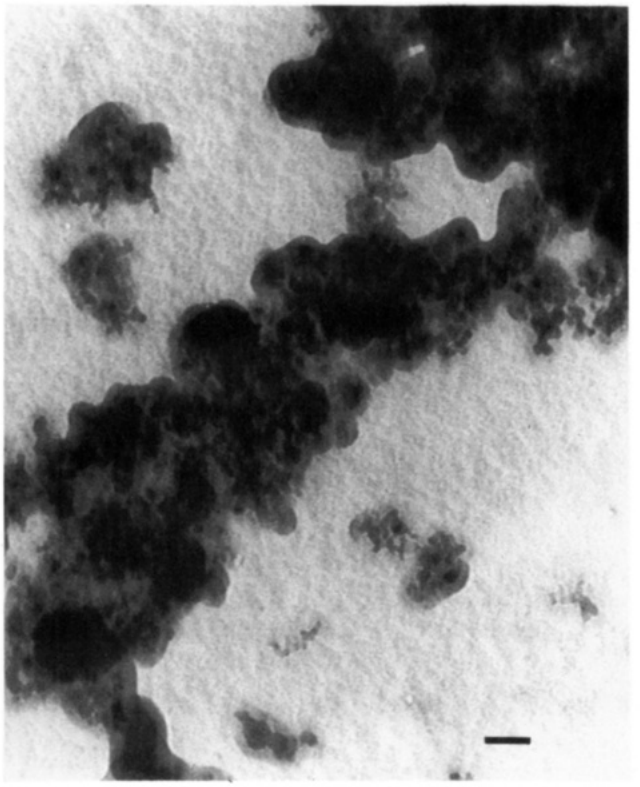

Figure 5. Replica of unfractionated ELPP, compression molded, 30-min Ar etch. Scale bar 50.0 nm.

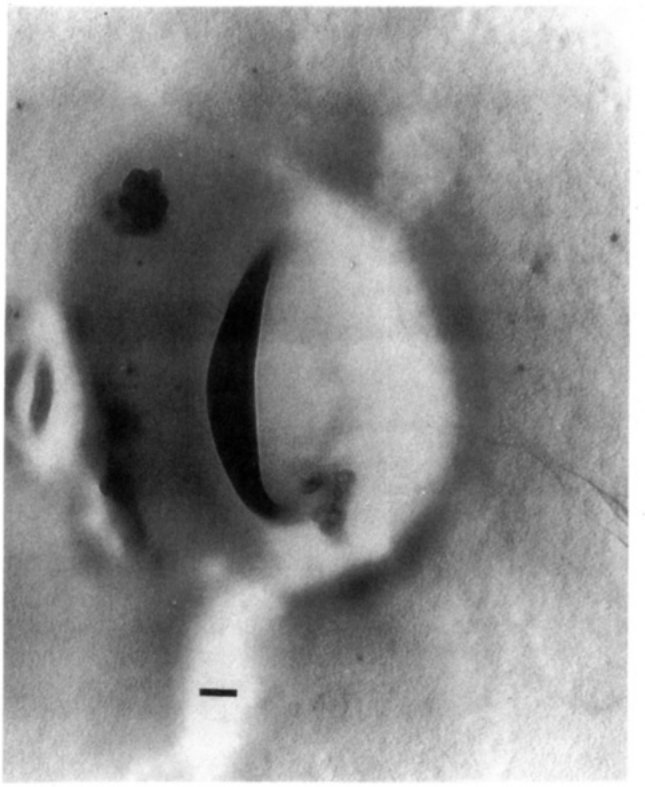

Figure 6. Replica of hexane-soluble ELPP fraction, compression molded, unetched. Scale bar 100 nm.

croscopy (TEM) analysis of argon ion etched fracture surfaces. In Figure 5, the TEM of a test specimen of unfractionated ELPP, a lamellar structure can be clearly seen as light wormlike structures, in addition to the residual alumina catalyst support. Lamellar thickness ranges from about 3.0 to 8.0 nm, with an estimated average thickness of about 4.0 nm. In addition to a distribution of lamellar thicknesses, the dimensions of the regions between the lamellae also seem to have a distribution of sizes, although it is difficult to assign numerical values to these dimensions. These darker regions presumably represent the amorphous regions in the polymer. The fairly broad range of lamellar thickness is consistent with the DSC data.

For the ether-soluble ELPP fraction, lamellar thicknesses were between 3.0 and 4.0 nm, and the thickness distribution was much narrower than that for the whole polymer. Since the repeat distance along the polypropylene helix in the isotactic I (monoclinic) unit cell is 0.65 nm/3 monomer unit,[15] chain segments having 14–18 monomer units in consecutive isotactic placement would fit into these crystallites.

In the hexane-soluble and -insoluble fractions, the lamellae were quite uniform in thickness, between 9.0 and 9.3 nm (Figures 6 and 7). Likewise, the regions between lamellae are smaller and more uniform in size compared to the whole polymer.

The test specimens, except for the ether-soluble fractions, had the same thermal history and should have the same lamellar thickness, if all other factors were the same. The thicker lamellae for the hexane-soluble and -insoluble fractions must reflect their higher average lengths of monomer units in isotactic placements. Both have essentially the same lamellar thickness because crystallization temperature, rather than isotactic block length, was limiting. The narrower size distribution for lamellar thickness and interlamellar size seen for the ELPP fractions, relative to the whole polymer, is a reflection of separating the polymer with low average isotactic block length from that with higher average block length.

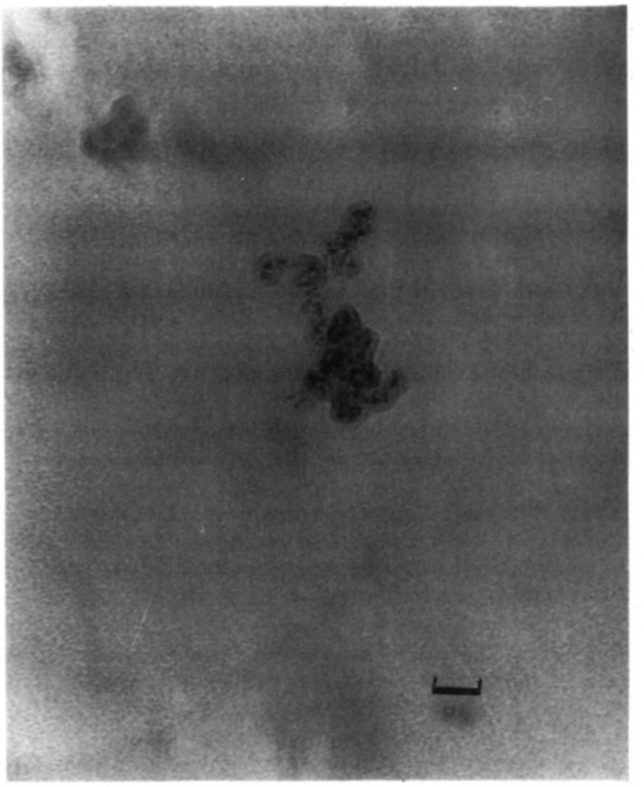

Figure 7. Replica of hexane-insoluble ELPP fraction, compression molded, unetched. Scale bar 50.0 nm.

Lamellar Thickness from DSC. It seems likely that the broad melting range seen in the DSC experiment corresponds to a broad range of crystallite sizes. In the case of highly isotactic polypropylene, thermal history determines average lamellar thickness. In the case of a stereoblock polymer such as ELPP, the isotactic block

Table V
Lamellar Thickness and Melting Temperature

sample	T_m, K	lamellar thickness, nm: calcd[a]	lamellar thickness, nm: obsd[b]
ELPP			
whole polymer	313–437	4.8–20	3.0–8.0
ether sol.	295–363	4.2–7.0	3.0–4.0
hexane sol.	313–403	4.8–11.9	9.0–9.3
hexane insol	313–439	4.8–45	9.0–9.3
Profax 6523	398–445	10–40	24

[a] From Figures 2 and 8. [b] From TEM.

length distribution may limit the number of lamellae of a given thickness that can form.

Lamellar size can also be estimated from DSC measurements. Many factors influence the melting temperature of lamellar crystallites. If all other variables are held constant, thinner lamellae will melt at lower temperatures than thicker lamellae. ELPP is a block, rather than random, copolymer, and DSC yields nonequilibrium melting data. Therefore, we have used a kinetic theory as developed by Hoffman and Lauritzen[16] and Price[17] rather than a thermodynamic approach to analyze the crystallization of ELPP.

The kinetic relationship, as given by Wunderlich[18] is

$$\langle l \rangle = \frac{2\sigma_e T_m^\circ M}{\rho_c \Delta H_f^\circ [T_m - T_m^\circ]} + \frac{kT_m}{b_0 \sigma_s} \qquad (9)$$

where $\langle l \rangle$ = average lamellar thickness, nm; σ_e = specific fold surface free energy = 100 mJ/m^2; T_m° = equilibrium melting temperature = 460.7 K; M = molecular weight of repeat unit = 42 g/mol; ρ_c = isotactic I crystal density = 0.94 g/cm^3; ΔH_f° = heat of fusion = 8.79 kJ/mol; T_m = observed melting temperature; k = Boltzmann's constant = 1.38×10^{-23} J/K; b_0 = single layer thickness = helix diameter = 0.65 nm; and σ_s = specific side surface free energy = 5 mJ/m^2. The melting temperature, heat of fusion, crystal density, and σ_e were suggested by Wunderlich.[3] The value of σ_s was arbitrarily taken to be the same as for polyethylene. Figure 8 is the resulting plot of lamellar thickness as a function of observed melting temperature.

The melting ranges observed in the DSC scans were used to obtain a predicted lamellar thickness from Figure 8. The calculated lamellar thicknesses and observed TEM thicknesses are given in Table V. Agreement is fair at large supercoolings (i.e., low melting temperatures), but the observed values at low supercoolings are considerably lower than predicted by eq 9. Two likely causes of this disagreement are recrystallization during the DSC scan and temperature dependence of the fold surface free energy, σ_e.

Recrystallization during the DSC experiment probably accounts for the fairly broad melting range observed for the commercial isotactic polypropylene, since the TEM of this material showed a uniform lamellar thickness of 24 nm. The observed lamellar thickness is halfway between the calculated thickness at the onset and end of the observed melting peak. It is normally observed that reducing the heating rate in a DSC experiment lowers the peak temperature and narrows the width of the peak.

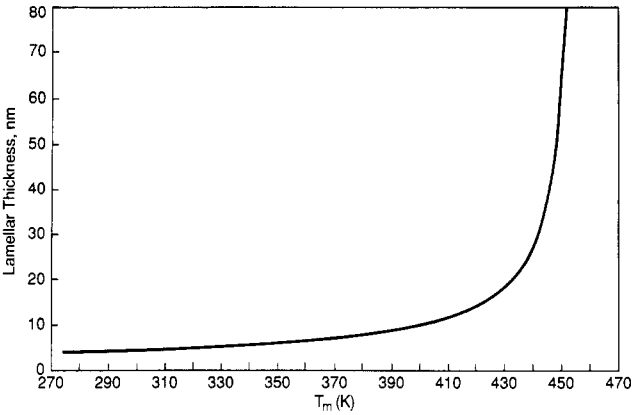

Figure 8. Lamellar thickness versus melting temperature, T_m, for polypropylene (eq 9).

In the case of ELPP and its fractions, lamellar size may be limited by both isotactic block length and crystallization temperature. The fold surface is also likely to be much more irregular, due to the wide isotactic block length distribution. This irregularity may lead to greater temperature dependence of σ_e for ELPP than for isotactic polypropylene.

Lamellar Thickness by Nitric Acid Etching. Further information about the relationship between DSC melting temperature and crystalline block length was obtained by nitric acid etching of ELPP. The technique depends upon the fact that chemical oxidants, such as nitric acid, attack the noncrystalline portions of polyolefins much more rapidly than the crystalline portions. It is possible to degrade selectively the noncrystalline portions and recover crystallites for further characterization.[19] The chief difficulty in applying the technique to ELPP was selection of an appropriate etching agent. The onset of melting of most ELPP samples was ca. 30 °C. The preferred etching agents, such as nitric acid, fuming nitric acid, and chromic–sulfuric acid do not attack polypropylene at a measurable rate below about 90 °C. To achieve reasonable rates, etching in nitric acid and fuming nitric acid was done at ca. 120 °C. Consequently, crystallites that melted at lower temperatures will have been destroyed, biasing the estimates to higher thicknesses.

Etching was performed on the test specimens with etch time as the experimental variable. The recovered crystalline portions were analyzed by gel permeation chromatography with the results shown in Table VI. As expected, the molecular weight of the residue decreased and the breadth of the distribution narrowed with etch time. Assuming that all of the recovered material was in the isotactic I crystal form, an average lamellar thickness was calculated from the molecular weight and the known

Table VI
Lamellar Thickness of Nitric Acid Etched ELPP

etch time, h	molec wt, GPC: $10^{-3}M_n$	molec wt, GPC: $10^{-3}M_w$	molec wt, GPC: M_w/M_n	calcd lamellar thickness, nm: av[a] no.	av[a] wt	DSC data[b] min	DSC data[b] max	DSC data[b] peak
1	4.85	13.0	2.64	25.0	67.1	10.1	24.0	16.9
2	2.31	8.20	3.54	11.9	42.3	6.5	15.0	12.5
3	1.32	2.42	1.83	6.8	12.5	8.0	12.8	11.2

[a] From molecular weights and the isotactic helical repeat distance of 0.65 nm/3 monomer residues. [b] From DSC minimum, maximum, and peak melting temperatures and Figure 8.

Table VII
Isotactic Block Distribution

fraction	$P(mm/m)$	% isotactic pentads	av N (≥4)
ELPP			
ether sol.	0.7	18	6.3
hexane sol.	0.85	40	9.7
hexane insol	0.92	70	15.5
isotactic PP	0.95–0.99		23–104

helical repeat distance of 0.65 nm/3 monomer residues.[3] Both the weight- and number-average molecular weights were used to estimate weight- and number-average lamellar thicknesses, respectively. For comparison, lamellar thicknesses were calculated from the DSC melting curves by using Figure 8.

For the narrow molecular weight distribution samples (3-h etch time), the DSC thicknesses calculated from the temperature of the onset of melting agree quite well with the thicknesses calculated from the number-average molecular weight, while the thicknesses calculated from the maximum melting temperature agree with those calculated from the weight-average molecular weight. This is reasonable since number-average molecular weight is a function of the total number of molecules being averaged, whereas weight-average molecular weight is dependent on the molecular weight of each molecule being averaged. Thus, the thickest and highest melting lamellae would contribute most to the weight-average molecular weight, while all of the lamellae would contribute to the number-average molecular weight. The lamellar thicknesses range from ca. 7 to 12.5 nm, corresponding to 32–58 monomer units in isotactic blocks, respectively.

Crystallinity of the ether-soluble fraction increased with molecular weight (Table IV). This is unusual, since at constant thermal history, polymer crystallizability tends to decrease with increasing molecular weight, due to increases in chain entanglement and reduced molecular mobility. In the case of ELPP, the number of long isotactic blocks appears to increase with molecular weight, facilitating cocrystallization. The lower crystallinity of the higher molecular weight hexane-soluble fraction may be due to incomplete fractionation caused by cocrystallization phenomenon in which less stereoregular material is insolubilized.

Polymer Microstructure Model. To test our postulate that the elasticity of ELPP is due to cocrystallization of a high molecular weight ether-soluble fraction,[1] we have estimated the effects of stereoregularity and molecular weight. The effect of regioisomerism being rather minor, we focus on the average size and size distribution of isotactic blocks.

We are particularly concerned with long isotactic blocks, and pentad data allow an estimate of blocks containing four or more monomer units in isotactic placements. The fraction of monomers in isotactic blocks containing four or more monomers is $n\ (\geq 4) = 2[rmmm] + [mmmm]$. The fractional number of isotactic blocks containing four or more monomer units is $b\ (\geq 4) = [rmmm]/2$. Therefore, the average length of isotactic blocks having four or more monomer units is

$$N\ (\geq 4) = n\ (\geq 4)/b\ (\geq 4) = 4 + 2[mmmm]/[rmmm] \tag{10}$$

This average block size depends only on the pentad distributions and can be verified from general expressions for average sequence lengths.[20]

Table VII summarizes the isotactic block sizes for the ELPP fractions and for isotactic polypropylenes. While in highly isotactic polypropylene the number-average length of isotactic blocks containing four or more monomers can exceed 100, the number-average length of such blocks is about 6 in the ELPP ether-soluble fraction, 10 in the hexane-soluble fraction, and 15 in the hexane-insoluble fraction.

A full description of the distribution of longer isotactic block lengths would require knowledge of the number of different catalysts sites and their selectivities. The number of sites is not known and their selectivities cannot be unequivocally determined from the pentad distributions. We assume a discrete number of sites and that the second-order Markov statistics of Table III provide a reasonable approximation to the sequence distributions of the fractions.

The sequence distributions up to hexads were calculated directly by using the computer program with the probabilities of Table III. Assuming that the probability of a meso insertion does not change after a given segment length (in this case, three monomer units) the relative number of longer isotactic sequences was calculated by repeated multiplication of the n-ad probabilities by $P(mm/m)$. The number of isotactic blocks containing four or more monomer units depends only on $P(mm/m)$. The values of the other probabilities, $P(mr/m)$, $P(rm/m)$, and $P(rr/m)$, are not critical, since they affect only the number of shorter isotactic blocks and the number of syndiotactic blocks. Thus, the model was also applied to the ether-soluble fraction, even though second-order Markov statistics did not give a good fit to its pentad distribution.

The relative number of isotactic sequences of length n will be defined as $N(m^n)$ and the corresponding relative number of blocks containing exactly $(n + 1)$ monomer units as $N(rm^nr)$. Then

$$N(rm^nr) = N(m^n) - N(m^{n+1}) \tag{11}$$

This follows from the fact that $N(m^n)$ contains contributions from sequences such as mm^nm, rm^nm, and rm^nr, while $N(m^{n+1})$ includes all of these, except rm^nr.

The relative number of monomer units in isotactic blocks containing $n + 1$ monomer units, $W(n + 1)$, is then given by

$$W(n + 1) = (n + 1)N(rm^nr) \tag{12}$$

$$W(n) = nN(rm^{n-1}r) \tag{13}$$

Since only isotactic blocks with $n \geq 5$ monomers contribute to the $mmmm$ pentad resonance, we calculate the weight of polymer in isotactic blocks exceeding a given length as a fraction of the total weight of polymer in isotactic blocks of five or more units, given by

$$F\ (\geq n) = \sum_{k=n}^{k=\infty} W(k) / \sum_{k=5}^{k=\infty} W(k) \tag{14}$$

Figure 9 shows the percent distribution of block sizes in the ELPP fractions with the second-order Markov statistics of Table III.

The formation of an elastic network by cocrystallization of isotactic blocks of stereoblock fractions requires two or more blocks of sufficient length per chain. This requirement can be satisfied only with a sufficiently high molecular weight of the fraction. The distributions in Figure 9 were used to calculate the weight percent of isotactic blocks for various block length intervals, i.e., 1–5, 6–10, 11–16, etc., monomer units for the ether-soluble and hexane-soluble fractions. Then the number of isotactic blocks per chain was calculated as a function of molecular weight and the average block length of the interval (Table VIII). The number of blocks per chain is highly sensitive

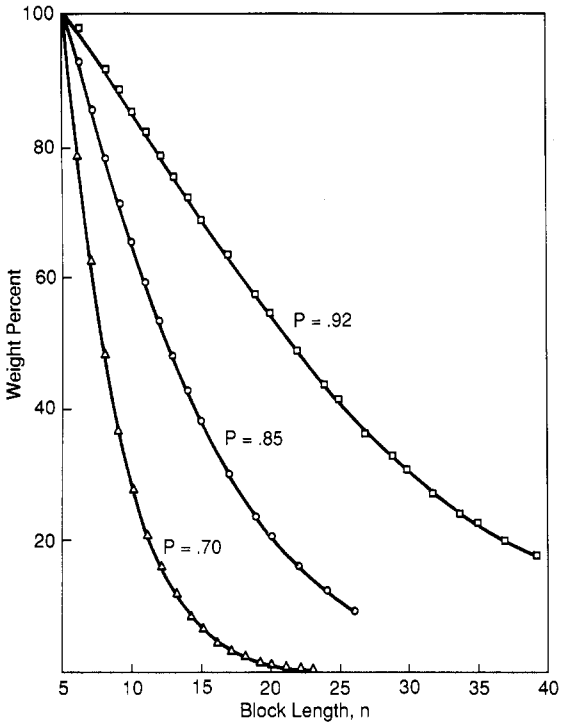

Figure 9. Weight percent polymer in isotactic blocks of length ≥ n monomer units for the ether-soluble, hexane-soluble, and hexane-insoluble fractions of ELPP with $P(mm/m)$ = 0.70, 0.85, and 0.92, respectively.

Table VIII
Number of Isotactic Blocks per Chain

block length range	hexane-sol. fractn		ether-sol. fractn	
	m blocks/ 100 000 DP	m blocks/ 100 000 mw	m blocks/ 100 000 DP	m blocks/ 100 000 mw
1–5	4371.0	103.9	3774.7	89.7
6–10	1004.0	23.9	296.3	7.0
11–15	380.0	9.0	43.1	1.0
16–20	156.0	3.7	6.7	0.2
21–25	65.9	1.6	1.1	0.0
26–30	28.2	0.7		
31–35	12.4	0.3		
36–40	5.5	0.1		
41–45	2.4	0.06		
46–50	1.5	0.04		
51–55	0.0	0.00		

to the isotacticity of the fraction and the block length interval (Figure 10).

Summary and Conclusions. The TEM studies of ELPP and its fractions suggest a morphology of cocontinuous hard and soft phases, much like that of segmented block copolymers such as the poly(ether esters).[21-23] The ELPP hard phase consists of crystalline isotactic polypropylene, and the soft phase of amorphous atactic polypropylene, perhaps with some crystallizable, but uncrystallized, isotactic blocks. Broad DSC melting curves indicate that the block length distribution is broad in both the hard and soft phases.

NMR studies of ELPP and solvent fractions indicate structure control by catalyst sites with a wide range of regio- and stereospecificities, resulting in fractions with isotacticities from 18 to >65%. The polymer microstructure is described approximately by second-order Markov statistics with different probabilities for each solvent fraction, which indicates a complex multiple-site catalyst system. Pentad sequence data cannot provide a uniquely better analysis.

The model based on the second-order Markov approximation helps confirm the postulate that the elastomeric

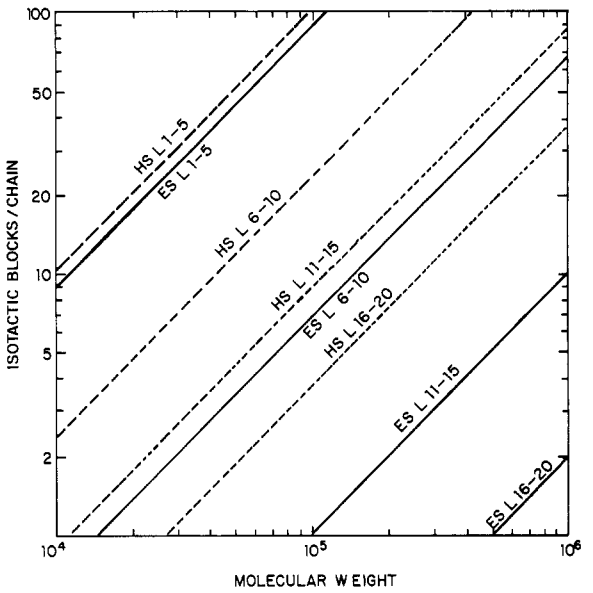

Figure 10. Number of isotactic blocks per chain as a function of block length and the molecular weight of the polymer fraction: (—) ether soluble (ES), P(mm/m) = 0.70, 18% isotactic pentads; (---) hexane soluble (HS), $P(mm/m)$ = 0.85, 40% isotactic pentads. L = block length range.

properties of ELPP are a consequence of the stereoblock character and high molecular weight of the ether-soluble fraction. The critical test is whether there are enough cocrystallizable isotactic blocks per chain to produce an elastic network via cocrystallization with the more stereoregular components. Estimates of the necessary isotactic block length come from the other characterization techniques.

The minimum crystalline lamellar thicknesses observed by TEM were 3 and 9 nm for the ether-soluble and hexane-soluble fractions, respectively (Table V). Nitric acid etching estimates were in the same range (Table VI). These thicknesses correspond to isotactic block lengths of 14 and 42 monomer units, respectively. The nitric acid etching estimates, and perhaps the TEM estimates, are probably biased toward larger lamellar thickness, but we conclude that cocrystallization requires isotactic block lengths on the order of 11–15 monomer units.

The model, Figure 10, indicates that the requirement of two or more blocks (of length 11–15) per chain is satisfied at a molecular weight of $\geq 2.2 \times 10^4$ for the hexane-soluble fraction and at $\geq 2.0 \times 10^5$ for the ether-soluble fraction, respectively. From the Mark–Houwink relationship[13] these values correspond to $\eta_{inh} \geq 0.3$ and 1.9 dL/g, respectively. Solvent fractionation data on typical ELPP's gave $\eta_{inh} \geq 2.5$ dL/g for these fractions (Table III, ref 1). Similarly, the number-average molecular weights were $\geq 2.6 \times 10^5$. Thus, the model is consistent with the observed data.

Elasticity measurements on blends of the ether-soluble fraction with Profax showed that the molecular weight of the fraction had to be greater than 2.5×10^5 to show elastic recovery.[1] This also indicates that the critical block length is on order of 11–15 and is consistent with the NMR model. In blends with lower molecular weight ether-soluble fractions, a plastic yield was observed in the stress–strain curve, suggesting phase incompatibility, as well as an insufficient number of cocrystallizable blocks.

Assuming that insolubilization is due to cocrystallization, the extraction studies provide an indirect measure of isotactic block size distribution. As shown in the accompanying paper, over 50% of an ether-soluble fraction with η_{inh} = 4.40 was not extractable with ether after melt

blending with Profax (Table V, ref 1). Further, the portion that was still soluble had an η_{inh} = 1.40. Thus, the insolubilized portion was much higher in molecular weight and would have had a larger number of isotactic blocks per chain.

The NMR rigidity results also revealed differences attributable to block size distributions. Cooling the solution of the ether-soluble fraction from 135 °C to room temperature reduced the observed isotactic pentad fraction 20%, whereas the decrease was 40% for the hexane-soluble fraction. The difference is an indication of a higher proportion of crystallizable blocks, i.e., there are more of the longer isotactic blocks in the hexane-soluble fraction.

Acknowledgment. Dr. H. Thielke and Ralph Fuller provided X-ray and GPC measurements, respectively. The NMR rigidity measurements were suggested and first tested by Dr. Fred Davidson. Helpful discussions with Profs. B. Wunderlich and U. Suter are gratefully acknowledged.

Registry No. ELPP, 9003-07-0.

References and Notes

(1) Collette, J. W.; Tullock, C. W.; MacDonald, R. N.; Buck, W. H.; Su, A. C. L.; Harrell, J. R.; Mulhaupt, R.; Anderson, B. C. Macromolecules, preceding paper in this issue.
(2) Luongo, J. P. *J. Appl. Polym Sci.* **1960**, *3*, 302.
(3) Wunderlich, B. *Macromolecular Physics*; Academic: New York, 1976; Vol. II, p 149; and private conversation.
(4) Asakura, T.; Ando, I.; Nishioka, A.; Doi, Y.; Keii, T. *Makromol. Chem.* **1977**, *178*, 791.
(5) Lindeman, L. P.; Adams, J. Q. *Anal. Chem.* **1971**, *43*, 1245.
(6) Cheng, H. N.; Bennett, M. A. "^{13}C NMR Spectra of Polyolefins". In *Advances in Polyolefins*; Seymour, R. B., Cheng, T., Eds.; Plenum Press: New York, 1987; p 393.
(7) Zambelli, A.; Locatelli, P.; Bajo, G.; Bovey, F. A. *Macromolecules* **1975**, *8*, 687.
(8) Stehling, F. C.; Knox, J. R. *Macromolecules* **1975**, *8*, 595.
(9) Zambelli, A.; Sacchi, M. C.; Locatelli, P. In *Transition Metal Catalyzed Polymerizations*; Quirk, R. P., Ed.; MMI Press Symposium Series, Vol. 4; Harwood Academic Publishers: New York, 1983; p 83.
(10) Doi, Y.; Suzuki, E.; Keii, T. Reference 9, p 737.
(11) Bovey, F. A. *High Resolution NMR of Macromolecules*; Academic Press: New York, 1972.
(12) Harwood, H. J. *J. Polym Sci, Part C* **1968**, *25*, 37; and private communications.
(13) Groenewege, M. P.; Schuyer, J.; Smidt, J.; Tuijnman, C. A. "Crystalline Olefin Polymers". In *High Polymers*; Raff, R. A. V., Doak, K. W., Eds.; Interscience: New York, 1965; Vol. XX, Part 1, pp 795–811.
(14) Cowie, J. M. G. *Eur. Polym. J.* **1973**, *91*, 1041.
(15) Aggarwal, S. L. In *Polymer Handbook*, 2nd Ed.; Bandrup, J., Immergut, E. H., Eds.; John Wiley & Sons: New York, 1975; p V-23.
(16) Lauritzen, J. I., Jr.; Hoffman, J. *J. Chem. Phys.* **1959**, *31*, 1680; *J. Res. Natl. Bur. Stand.* **1959**, *64A*, 73.
(17) Price, F. P. *J. Chem. Phys.* **1959**, *31*, 1679.
(18) Wunderlich, B. *Macromolecular Physics*; Academic: New York, 1973; Vol. I, p 388.
(19) Hock, C. W. *J. Polym. Sci.: B* **1965**, *3*, 573; *J. Polym. Sci.: A-2* **1966**, *4*, 227.
(20) Randall, J. C. *J. Polym. Sci., Polym. Phys. Ed.* **1976**, *14*, 2083.
(21) Cella, R. J. *J. Polym. Sci., Symp.* **1973**, *42*, 737.
(22) Buck, W. H.; Cella, R. J.; Gladding, E. K.; Wolfe, J. R. *J. Polym. Sci., Symp.* **1974**, *48*, 47.
(23) Cella, R. J. *Encyclopedia of Polymer Science and Technology*; John Wiley and Sons: New York, 1977; Supplement Vol. 2, p 485.

Laser-Pulsed Photopolymerization of Methyl Methacrylate: The Effect of Repetition Rate

Charles E. Hoyle,* M. A. Trapp, C. H. Chang, D. D. Latham, and Kevin W. McLaughlin

Department of Polymer Science, University of Southern Mississippi, Hattiesburg, Mississippi 39406-0076. *Received September 12, 1988; Revised Manuscript Received January 31, 1989*

ABSTRACT: The photopolymerization of neat methyl methacrylate at several different photoinitiator optical densities has been completed using a pulsed excimer laser. The operation of the laser was controlled using a microcomputer with the capability of firing the laser in two different modes. The first mode (single-pulse mode) was a continuous pulsing with each pulse separated by a 10-s time interval. This gave, upon GPC analysis, a broad molecular weight distribution. The second mode of pulsing (double-pulse mode), a sequence of two pulse blocks with a time between pulses of 100 ms and a time between the blocks of 10 s, gave a complex distribution characterized by a narrow shoulder superimposed on a broad molecular weight distribution. Both distributions can be described by employing the use of generating functions to solve the basic kinetic equations of polymerization.

Introduction

There has been a recent surge of interest in the use of lasers as a source to initiate free-radical polymerization processes.[1-31] Experiments have been directed at using lasers as both unique flash lamp sources to gain critical information dealing with the kinetics of free-radical polymerization processes and as a basic evaluation of laser sources as means of generating polymers with specific properties. In view of the obvious interest in laser-initiated polymerization processes, it is worthwhile to consider the kinetics of the polymerization and the molecular weight distributions derived therefrom.

Olaj and co-workers[8-12] have presented an evaluation of the rate constants of styrene using a "pseudostationary" approximation to describe the polymerization process. In this paper, we present experimental results for the laser-initiated polymerization of neat methyl methacrylate under a variety of considerations. By operation of the laser in both a "single-pulse" and "double-pulse" mode, two distinct and quite different molecular weight distributions are produced. The shape of the distributions are described

* Author to whom correspondence should be directed.

0024-9297/89/2222-3866$01.50/0